An Analysis of the *m*-Port Symmetrical *H*-Plane Waveguide Junction with Central Ferrite Post*

J. B. DAVIES†

Summary—An analysis is presented for the *m*-port symmetrical *H*-plane waveguide junction with central ferrite post. It has application to the engineering problem of microwave circulators and to the more academic problem of the empty symmetrical junction. An exact solution is formulated from which is developed an approximation that is equivalent to considering only the propagating modes of the rectangular waveguides. The method is found to give results in agreement with the theory for the 2-port junction (*i.e.*, waveguide) with ferrite post, and with experiment for ferrite-free 3- and 4-port junctions. Theoretical design curves are given for the 3-port circulator, although for lack of suitable ferrite data, these have not been checked accurately. A number of 3- and 4-port circulators have been made to designs arising from the analysis. Because the microwave performance is derived explicitly in terms of the junction geometry and ferrite properties, the design of a particular component must of necessity involve much computation.

I. Introduction

A COMPONENT of great use to the microwave engineer is the 3- or 4-port circulator, in which a wave entering port 1 emerges from port 2, and so on in a cyclic manner. A particularly compact form of circulator is in the form of a symmetrical *Y* or cross junction of waveguides with a magnetized ferrite post mounted centrally in the junction.[1–3] These circulators have been developed over the last 3 or 4 years purely by experiment, with very little understanding of their mode of operation.

The method of analysis adopted here is to match exactly each cylindrical mode in the ferrite post to the associated mode outside the post, which in turn is matched exactly to the complete set of modes of the rectangular waveguide. An infinity of equations results (one for each cylindrical mode), each involving an infinity of unknowns (the amplitudes of the rectangular waveguide modes). An approximation to this infinite linear system is then developed in detail that is equivalent to ignoring the evanescent modes of the rectangular waveguide. By considering solutions that correspond to each eigenvector in turn of the scattering matrix, only the fields of one of the *m* waveguides need be matched in the above procedure.

We consider a junction of *m* rectangular waveguides spaced equally around the junction axis. These identical waveguides are supposed capable of propagating only the TE_{10} mode, with the electric field in the direction of the symmetry axis. A full-height circular cylinder of gyromagnetic material is placed at the center of the junction with its gyroaxis along the junction axis of symmetry. With specified waveguide terminal planes, the problem is to derive the scattering matrix of this *m*-port symmetrical junction. From the outset we assume there to be no losses in the junction.

II. The Scattering Matrix[4]

Take the waveguide terminal planes to be equidistant from the junction axis, this distance being half an integral number of guide wavelengths. The planes are sufficiently far from the junction that fields there are due only to the propagating modes. Let a_i represent the transverse electric field of the incoming wave at the terminal plane of the ith port, the ports being numbered consecutively around the junction. Let b_i similarly represent the outgoing wave. If $\boldsymbol{a}$ and $\boldsymbol{b}$ are column vectors with elements a_i and b_i respectively, then $\boldsymbol{b}=S\boldsymbol{a}$ defines the scattering matrix S. From the symmetry property of the junction, the scattering matrix must have eigenvectors $\boldsymbol{v}_0, \boldsymbol{v}_1, \cdots, \boldsymbol{v}_{m-1}$, where $\boldsymbol{v}_j$ is a column vector with elements $\exp(2\pi ij/m)$, $\exp(4\pi ij/m)$, $\exp(6\pi ij/m)$, $\cdots 1$. If the corresponding eigenvalues are λ_0,[5] $\lambda_1, \cdots, \lambda_{m-1}$, then the scattering matrix is given by:

$$S = \begin{bmatrix} s_0 & s_1 & s_2 \cdots s_{m-1} \\ s_{m-1} & s_0 & s_1 \cdots s_{m-2} \\ \cdot & \cdot & \cdot \cdot \cdot \cdot \cdot \\ s_1 & s_2 & s_3 \cdots s_0 \end{bmatrix}, \tag{1}$$

where

$$s_j = \frac{1}{m} \sum_{k=0}^{m-1} \lambda_k \exp(-2\pi ijk/m). \tag{2}$$

For the loss-free junction being considered, S must be unitary, and so have all its eigenvalues on the unit

* Received March 19, 1962; revised manuscript received, August 16, 1962. Mullard Research Laboratories, Redhill, Surrey, Eng., Rept. No. 406.

† Systems Division, Mullard Research Laboratories, Redhill, Surrey, England.

[1] H. N. Chait and T. R. Curry, "Y circulator," *J. Appl. Phys.*, Supplement to vol. 30, pp. 152S–153S; April, 1959.

[2] B. A. Auld, "The synthesis of symmetrical waveguide circulators," IRE Trans. on Microwave Theory and Techniques, vol. MTT-7, pp. 244–245; April, 1959.

[3] P. E. V. Allin and F. W. Smith, "Waveguide circulators," Brit. Patent Specification No. 852,751; Application Date December 2, 1957.

[4] C. G. Montgomery, R. H. Dicke, and E. M. Purcell, "Principles of Microwave Circuits," McGraw-Hill Book Co., Inc., New York, N. Y., chs. 5 and 12; 1948.

[5] No confusion should arise from the use of λ_0 for an eigenvalue and for the free-space wavelength, if only because of their dimensional difference.

circle. The behavior of the nonreciprocal m-port symmetrical junction is therefore described by just m figures, say the arguments of the m eigenvalues. The m-port symmetrical junction will be a circulator if all the elements $s_0, s_1, \cdots, s_{m-1}$, but one, say s_u, are zero, u being non-zero. By (2) this corresponds to eigenvalues having values:

$$\lambda_k = \lambda_0 \exp(2\pi iku/m). \qquad (3)$$

The junction is an m-port circulator if, in addition, u is prime to m. For example, the 6-port junction is a 6-port circulator if the only nonzero element is either s_1 or s_5. If only s_2 or s_4 is nonzero we have two distinct 3-port circulators, whilst if only s_3 is nonzero we have three distinct 2-port circulators. The latter are, of course, loss-free 2-port networks with zero reflection coefficient.

From the relation $Sv_j = \lambda_j v_j$ we note that v_j represents a possible field excitation in the junction with the same reflection coefficient $1/\lambda_j$ at each terminal plane. The electric fields at the terminal planes will then be proportional to the elements of the respective eigenvector v_j.

III. Field Analysis

Circular cylindrical and rectangular coordinate systems (r, ϕ, z) and (x, y, z), are employed (see Fig. 1), the z axis coinciding with the junction axis of symmetry. The longitudinal axis of a particular waveguide is taken as $\phi = 0$ and $y = 0$. The ferrite post radius is R and the waveguide width is $2a$.

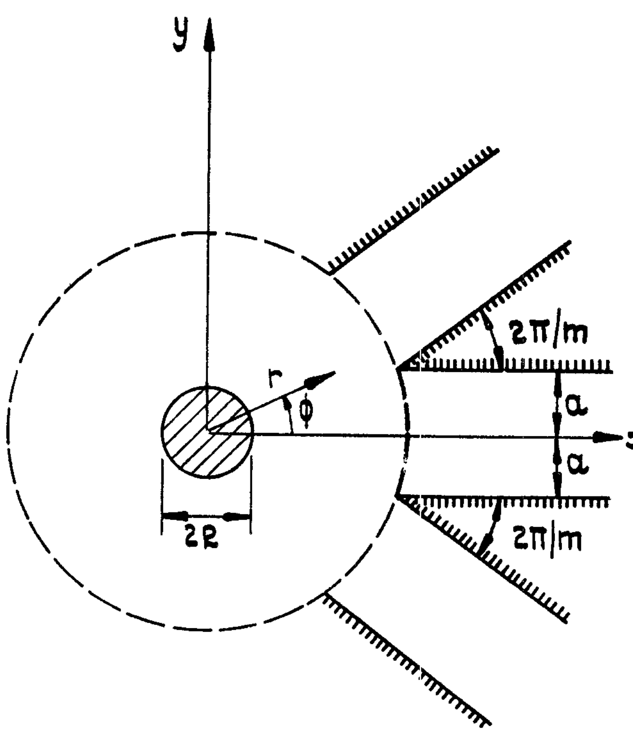

Fig. 1—Configuration of ferrite post in the m-port waveguide junction.

Because fields throughout the junction are excited by TE_{10} modes at the terminal planes, and as there are no z-dependent boundary conditions, we seek solutions with electric fields purely in the z direction and magnetic fields purely in the x-y plane. The fields are independent of z and are taken to have time dependence $\exp(i\omega t)$. A complete expansion for fields in the ferrite is therefore[6]

$$E_z = \sum_{n=-\infty}^{\infty} A_n J_n(\gamma r) \exp(-in\phi), \qquad (4)$$

$$H_\phi = -\frac{i}{\omega(\mu^2 - \kappa^2)} \sum_{n=-\infty}^{\infty} \left\{ \mu\gamma \; A_n J_n'(\gamma r) + \frac{\kappa}{r} A_n n J_n(\gamma r) \right\} \exp(-in\phi), \qquad (5)$$

$$H_r = \frac{1}{\omega(\mu^2 - \kappa^2)} \sum_{n=-\infty}^{\infty} \left\{ \kappa\gamma \; A_n J_n'(\gamma r) + \frac{\mu}{r} A_n n J_n(\gamma r) \right\} \exp(-in\phi), \qquad (6)$$

$$E_r = E_\phi = H_z = 0, \qquad (7)$$

where

$$\gamma^2 = \frac{\omega^2 \epsilon(\mu^2 - \kappa^2)}{\mu},$$

ϵ is the ferrite permittivity, and

$$\begin{pmatrix} \mu & -i\kappa \\ i\kappa & \mu \end{pmatrix}$$

is the ferrite permeability tensor in the x-y plane.

Similarly fields outside the ferrite $(r \geq R)$ are of the form

$$E_z = \sum_{n=-\infty}^{\infty} \{ B_n J_n(\gamma_0 r) + C_n Y_n(\gamma_0 r) \} \exp(-in\phi), \qquad (8)$$

$$H_\phi = -i\sqrt{\frac{\epsilon_0}{\mu_0}} \sum_{n=-\infty}^{\infty} \{ B_n J_n'(\gamma_0 r) + C_n Y_n'(\gamma_0 r) \} \cdot \exp(-in\phi), \qquad (9)$$

$$H_r = \frac{1}{\omega\mu_0 r} \sum_{n=-\infty}^{\infty} n \{ B_n J_n(\gamma_0 r) + C_n Y_n(\gamma_0 r) \} \cdot \exp(-in\phi), \qquad (10)$$

$$E_r = E_\phi = H_z = 0, \qquad (11)$$

where $\gamma_0^2 = \omega^2 \mu_0 \epsilon_0$.

[6] P. S. Epstein, "Theory of wave propagation in a gyromagnetic medium," *Rev. Mod. Phys.*, vol. 28, pp. 3–17; January, 1956. (See especially Section 6.)

Continuity conditions on E_z and H_ϕ can be applied at $r=R$ to the individual modes of the above series to give

$$A_n J_n(\gamma R) = B_n J_n(\gamma_0 R) + C_n Y_n(\gamma_0 R), \tag{12}$$

$$\frac{\epsilon\gamma_0}{\epsilon_0\gamma}\left\{J_n'(\gamma R) + \frac{\kappa n}{\mu\gamma R}J_n(\gamma R)\right\}A_n = B_n J_n'(\gamma_0 R) + C_n Y_n'(\gamma_0 R), \tag{13}$$

from which

$$\frac{C_n}{B_n} = -\frac{J_n(\gamma_0 R)}{Y_n(\gamma_0 R)} \cdot \frac{\left\{\left[\frac{J_n'(\gamma R)}{\gamma R J_n(\gamma R)} + \frac{\kappa n}{\mu(\gamma R)^2}\right]\frac{\epsilon}{\epsilon_0} - \frac{J_n'(\gamma_0 R)}{\gamma_0 R J_n(\gamma_0 R)}\right\}}{\left\{\left[\frac{J_n'(\gamma R)}{\gamma R J_n(\gamma R)} + \frac{\kappa n}{\mu(\gamma R)^2}\right]\frac{\epsilon}{\epsilon_0} - \frac{Y_n'(\gamma_0 R)}{\gamma_0 R Y_n(\gamma_0)}\right\}}. \tag{14}$$

We now consider fields throughout the m-port junction due to excitation of one particular eigenvector of the scattering matrix. We noted earlier that an eigensolution is excited by electric fields at the terminal planes that are proportional to the elements of the corresponding eigenvector. It follows that if $E_z^j(r, \phi)$ denotes the electric field of the jth eigensolution, then

$$E_z^j(r, \phi) = \exp(2\pi i j/m) E_z^j(r, \phi + 2\pi/m). \tag{15}$$

Hence for the jth eigensolution the various field components inside and outside of the ferrite will be given by (4)–(7) and (8)–(11), with summation over $n=mq+j$ for $q=0, \pm 1, \pm 2, \cdots$ instead of $n=0, \pm 1, \pm 2, \cdots$. By treating the eigensolutions individually, and because of (15), it is sufficient to consider the fields in one waveguide together with the sector joining it to the junction axis, as shown in Fig. 1.

A complete expansion for the fields in the waveguide is:

$$E_z = \sum_{p=-1}^{\infty} D_p \sin\left[\frac{(1+y/a)p\pi}{2}\right]\cdot\exp(i\beta_p x) \tag{16}$$

$$H_x = \frac{i\pi}{2\omega\mu_0 a}\sum_{p=-1}^{\infty} pD_p \cos\left[\frac{(1+y/a)p\pi}{2}\right]\exp(i\beta_p x) \tag{17}$$

$$H_y = \frac{1}{\omega\mu_0}\sum_{p=-1}^{\infty} D_p\beta_p \sin\left[\frac{(1+y/a)p\pi}{2}\right]\exp(i\beta_p x), \tag{18}$$

where

$$\beta_1 = \sqrt{\{\omega^2\mu_0\epsilon_0 - (\pi/2a)^2\}} = 2\pi/\lambda_g \tag{19}$$

$$\beta_{-1} = -\beta_1 \tag{20}$$

and

$$\beta_p = i\sqrt{\{(p\pi/2a)^2 - \omega^2\mu_0\epsilon_0\}} \quad \text{for } p \geq 2. \tag{21}$$

λ_g is the guide wavelength of the TE_{10} mode.

D_1 and D_{-1} are field amplitudes of the inward and outward traveling waves, referred to $x=0$ or equivalently to the terminal plane. If the above fields correspond to excitation of the jth eigensolution, then the eigenvalue is $\lambda_j = -D_{-1}/D_1$.

We now match the fields of (8) and (9) with the waveguide fields of (16) to (18) along the arc of radius $a/\sin(\pi/m)$. Equating E_z from (8) and (16), multiplying by $\exp(in\phi)$ and integrating from $-\pi/m$ to π/m gives

$$B_n J_n\left[\frac{\gamma_0 a}{\sin(\pi/m)}\right] + C_n Y_n\left[\frac{\gamma_0 a}{\sin(\pi/m)}\right] = \frac{m}{2\pi}\int_{-\pi/m}^{\pi/m}\exp(in\phi)\sum_{p=-1}^{\infty} D_p \sin\left\{\frac{p\pi}{2}\left[1 + \frac{\sin\phi}{\sin(\pi/m)}\right]\right\}\cdot\exp\left[\frac{i\beta_p a\cos\phi}{\sin(\pi/m)}\right]d\phi. \tag{22}$$

Similarly matching H_ϕ to $(H_y\cos\phi - H_x\sin\phi)$ gives

$$B_n J_n'\left[\frac{\gamma_0 a}{\sin(\pi/m)}\right] + C_n Y_n'\left[\frac{\gamma_0 a}{\sin(\pi/m)}\right] = \frac{m}{2\pi\omega\sqrt{(\mu_0\epsilon_0)}}\int_{-\pi/m}^{\pi/m}\cdot\exp(in\phi)\sum_{p=-1}^{\infty} D_p\left\{i\beta_p\cos\phi\sin\left[\frac{p\pi}{2}\left(1+\frac{\sin\phi}{\sin(\pi/m)}\right)\right] + \frac{p\pi}{2a}\sin\phi\cos\left[\frac{p\pi}{2}\left(1+\frac{\sin\phi}{\sin(\pi/m)}\right)\right]\right\}\cdot\exp\left[\frac{i\beta_p a\cos\phi}{\sin(\pi/m)}\right]d\phi. \tag{23}$$

Eqs. (22) and (23) can be combined as

$$\sum_{p=-1}^{\infty} D_p\int_{-\pi/m}^{\pi/m}\exp\left[\frac{i\beta_p a\cos\phi}{\sin(\pi/m)}\right]\cdot\left\{\sin\left(\frac{p\pi}{2}\right)\cos n\phi\left[\frac{i\beta_p\lambda_0}{2\pi}\cos\phi\cos\left(\frac{p\pi\sin\phi}{2\sin(\pi/m)}\right) - \frac{p\lambda_0}{4a}\sin\phi\sin\left(\frac{p\pi\sin\phi}{2\sin(\pi/m)}\right) - S_n^m\cos\left(\frac{p\pi\sin\phi}{2\sin(\pi/m)}\right)\right] + i\cos\left(\frac{p\pi}{2}\right)\sin n\phi\left[\frac{i\beta_p\lambda_0}{2\pi}\cos\phi\sin\left(\frac{p\pi\sin\phi}{2\sin(\pi/m)}\right) + \frac{p\lambda_0}{4a}\sin\phi\cos\left(\frac{p\pi\sin\phi}{2\sin(\pi/m)}\right) - S_n^m\sin\left(\frac{p\pi\sin\phi}{2\sin(\pi/m)}\right)\right]\right\}d\phi = 0, \tag{24}$$

where

$$S_n^m = \frac{J_n'\left[\frac{\gamma_0 a}{\sin(\pi/m)}\right] + \frac{C_n}{B_n}Y_n'\left[\frac{\gamma_0 a}{\sin(\pi/m)}\right]}{J_n\left[\frac{\gamma_0 a}{\sin(\pi/m)}\right] + \frac{C_n}{B_n}Y_n\left[\frac{\gamma_0 a}{\sin(\pi/m)}\right]}. \tag{25}$$

Eq. (24) involves an infinity of unknown coefficients D_p, the waveguide mode amplitudes, and in considering the jth eigensolution, the equation must be satisfied for $n=mq+j$, where $q=0, \pm 1, \pm 2, \cdots$. For each eigensolution we therefore have an infinite linear system of equations relating the coefficients D_p, of which only the ratio D_{-1}/D_1 is required. This infinite linear system is a precise formulation of the junction problem, the analysis so far being exact.

Letting $G_p=D_p[\sin(p\pi/2)+i\cos(p\pi/2)]$, the system of (24) can be written

$$\sum_{p=-1}^{\infty} A_p(q)\cdot G_p = 0 \qquad q=0, \pm 1, \pm 2, \cdots, \quad (26)$$

where, for p odd

$$A_p(q) = \int_0^{\pi/m} \exp\left[\frac{i\beta_p a\cos\phi}{\sin(\pi/m)}\right]\cos[(mq+j)\phi] \cdot\left\{\frac{i\beta_p\lambda_0}{2\pi}\cos\phi\cos\left[\frac{p\pi\sin\phi}{2\sin(\pi/m)}\right] - \frac{p\lambda_0}{4a}\sin\phi\sin\left[\frac{p\pi\sin\phi}{2\sin(\pi/m)}\right] - S^m_{mq+j}\cos\left[\frac{p\pi\sin\phi}{2\sin(\pi/m)}\right]\right\}d\phi, \quad (27)$$

and for p even

$$A_p(q) = \int_0^{\pi/m} \exp\left[\frac{i\beta_p a\cos\phi}{\sin(\pi/m)}\right]\sin[(mq+j)\phi] \cdot\left\{\frac{i\beta_p\lambda_0}{2\pi}\cos\phi\sin\left[\frac{p\pi\sin\phi}{2\sin(\pi/m)}\right] + \frac{p\lambda_0}{4a}\sin\phi\cos\left[\frac{p\pi\sin\phi}{2\sin(\pi/m)}\right] - S^m_{mq+j}\sin\left[\frac{p\pi\sin\phi}{2\sin(\pi/m)}\right]\right\}d\phi. \quad (28)$$

Now take the leading $2r+1$ terms of (26) for $q=0, \pm 1, \cdots, \pm r$, and solve for G_{-1}/G_1

$$\frac{G_{-1}}{G_1} = \frac{-\begin{vmatrix} A_1(r) & A_2(r) & \cdots & A_{2r+1}(r) \\ A_1(r-1) & A_2(r-1) & \cdots & A_{2r+1}(r-1) \\ & & \cdots & \\ A_1(-r) & A_2(-r) & \cdots & A_{2r+1}(-r) \end{vmatrix}}{\begin{vmatrix} A_{-1}(r) & A_2(r) & \cdots & A_{2r+1}(r) \\ A_{-1}(r-1) & A_2(r-1) & \cdots & A_{2r+1}(r-1) \\ & & \cdots & \\ A_{-1}(-r) & A_2(-r) & \cdots & A_{2r+1}(-r) \end{vmatrix}}. \quad (29)$$

Successive approximate solutions to the infinite system can be derived from one of the linear equations, from three equations and so on, the $(r+1)$th iterate being given by (29). We note that $A_p(q)$ is real for all but $p=\pm 1$, and that $A_1^*(q)=A_{-1}(q)$. As a result, only one of the above two determinants need be evaluated for any iterate, and further, each approximation to $\lambda_j=G_{-1}/G_1$ in fact has unit magnitude, a condition on the eigenvalues of the loss-free junction.

The remainder of this analysis is devoted to the first of the above approximations, namely $\lambda_j=-A_1(q)/A_1^*(q)$, but with q now chosen to minimize $|mq+j|$. When m is even, $j=m/2$ allows q to be -1 or 0, and as these will generally give different results, we will take the mean value of the eigenvalue arguments. This procedure is adopted because cylindrical modes with $\exp(im\phi/2)$ and $\exp(-im\phi/2)$ dependence must always be equally excited, so that no priority can be assigned to either of the results $n=\pm m/2$. However, for other eigensolutions of the scattering matrix, we can clearly expect the best approximation by consideration of the lowest possible order of cylindrical mode.

Compared with the exact analysis culminating in the limit of (29) with infinite determinants, the adopted approximation is equivalent to ignoring the evanescent modes of the rectangular waveguide arms. No approximation is made on the cylindrical modes, which are matched individually at the surface of the ferrite post and at the join of the waveguide arm to the central junction.

Defining θ_j by $\lambda_j=\exp(i\theta_j)$, the approximation takes the form

$$\tan\tfrac{1}{2}(\theta_j+\pi) = \frac{\mathrm{Im}[A_1(q)]}{\mathrm{Re}[A_1(q)]} = \left\{\frac{D_n^m + E_n^m(C_n/B_n)}{F_n^m + G_n^m(C_n/B_n)}\right\}, \quad (30)$$

where

$$D_n^m = -J_n(L)\int_0^{\pi/m}\cos n\phi \cdot\{\cos\phi\cos(M\cos\phi)\cos(N\sin\phi)\lambda_0/\lambda_g - \sin\phi\sin(M\cos\phi)\sin(N\sin\phi)\lambda_0/4a\}d\phi + J_n'(L)\int_0^{\pi/m}\cos n\phi\sin(M\cos\phi)\cdot\cos(N\sin\phi)d\phi, \quad (31)$$

$$E_n^m = -Y_n(L)\int_0^{\pi/m}\cos n\phi \cdot\{\cos\phi\cos(M\cos\phi)\cos(N\sin\phi)\lambda_0/\lambda_g - \sin\phi\sin(M\cos\phi)\sin(N\sin\phi)\lambda_0/4a\}d\phi + Y_n'(L)\int_0^{\pi/m}\cos n\phi\sin(M\cos\phi)\cdot\cos(N\sin\phi)d\phi, \quad (32)$$

$$F_n{}^m = J_n(L) \int_0^{\pi/m} \cos n\phi \cdot \{\cos\phi \sin(M\cos\phi)\cos(N\sin\phi)\lambda_0/\lambda_g + \sin\phi\cos(M\cos\phi)\sin(N\sin\phi)\lambda_0/4a\} d\phi + J_n'(L)\int_0^{\pi/m} \cos n\phi \cos(M\cos\phi) \cdot \cos(N\sin\phi) d\phi, \quad (33)$$

$$G_n{}^m = Y_n(L) \int_0^{\pi/m} \cos n\phi \cdot \{\cos\phi \sin(M\cos\phi)\cos(N\sin\phi)\lambda_0/\lambda_g + \sin\phi\cos(M\cos\phi)\sin(N\sin\phi)\lambda_0/4a\} d\phi + Y_n'(L)\int_0^{\pi/m} \cos n\phi \cos(M\cos\phi) \cdot \cos(N\sin\phi) d\phi, \quad (34)$$

where

$$L = \frac{2\pi a}{\lambda_0 \sin(\pi/m)} \quad (35)$$

$$M = \frac{2\pi a}{\lambda_g \sin(\pi/m)} \quad (36)$$

$$N = \frac{\pi}{2\sin(\pi/m)} \quad (37)$$

and $n = mq+j$, the integer q being chosen to minimize $|mq+j|$.

Eq. (30) is in a form convenient for computing, in that C_n/B_n is a function only of the ferrite properties and radius [by (14)], whilst $D_n{}^m$, $E_n{}^m$, $F_n{}^m$ and $G_n{}^m$ are functions only of the basic waveguide (m and λ_0/a). For the empty waveguide junction C_n/B_n is zero for all n, and the factors $D_n{}^m$ and $F_n{}^m$ alone will give the (approximate) scattering matrix.

The factors D, E, F and G involve definite integrals that are generally unrelated to tabulated functions, and so the integrals have been evaluated on a high-speed computer for $m=2$, 3 and 4 with a corresponding range of n. A wide range of frequencies was covered for $m=3$ and 4 but only the case $\lambda_g = 4a$ for $m=2$. D, E, F and G have so been derived, and are tabulated in the Appendix for the case $\lambda_g = 4a$. For $\lambda_g = 4a$, all the definite integrals for $m=4$ (and a number of integrals for $m=2$) can be related to Bessel and Struve functions of half integral order. These involved relationships have enabled a number of checks to be made on the computations.

IV. Testing of the Analysis

Having derived an approximate solution for the scattering matrix, we must now test its accuracy. It has already been noted that the approximation gives eigenvalues that lie on the unit circle, where indeed they must lie for a loss-free junction. It should also be noted that if the ferrite is isotropic, so that $C_j/B_j = C_{-j}/B_{-j}$ for all j, then the eigenvalues λ_j and λ_{m-j} coalesce. This again is as it should be, the reciprocal symmetrical m-port junction having a symmetric scattering matrix, which corresponds by (2) to the same eigenvalue degeneracies.

To assess the accuracy of the analysis, a comparison has been made with experiment for the empty 4-port and 3-port junction, and the 4-port junction with central conducting post. The analysis has also been compared with previous theory for the thin ferrite post in the 2-port junction. The 4- and 3-port junctions were measured free of ferrite because of the far greater experimental accuracy that can be achieved. Ferrite loading would introduce significant losses into the junction, and involve factors μ, κ and ϵ that are not known with adequate accuracy. In that the cylindrical modes are matched exactly at the ferrite surface, whereas the approximation involves ignoring the evanescent modes in the rectangular waveguide, it is expected that the approximation has the same order of accuracy for the reciprocal junction as for the junction with ferrite loading. Theory and experiment have also been compared with ferrite loaded junctions and are referred to in Section V. Although there is fair agreement, the comparison cannot be precise in view of the relatively imprecise knowledge of the ferrite properties.

A. Results

All eigenvalues are described in terms of their arguments, *i.e.*, $\lambda_j = \exp(i\pi\theta_j/180)$ where the θ's are now in degrees. Experimental results have a probable error of about $\pm 2°$ and were derived by the straightforward technique employing a standing-wave indicator at one port and calibrated variable short-circuits at all other ports. When there are nulls of electric field in all the waveguides at the same distance d from the symmetry axis, the argument of the corresponding eigenvalue is given by $\theta = (d/\lambda_g)\ 720° + (2v+1)\ 180°$, v being an integer. The reciprocal 3- and 4-port junctions each have a two-fold degeneracy of eigenvalues, and these were also measured by adjusting a short-circuit at port 3 so that no power travels to port 2 from port 1. In this precise experiment (described by Dicke[7] for the 3-port junction), the eigenvectors $(1, 0, -1)$ for the 3-port and $(1, 0, -1, 0)$ for the 4-port are excited, being linear combinations of the eigenvectors $(1, \omega, \omega^2)$ and $(1, \omega^2, \omega)$ or $(1, i, -1, -i)$ and $(1, -i, -1, i)$ used in Section II.

1) Empty 3- and 4-Port Junctions:

Theoretical and experimental values of the eigenvalue arguments are compared in Figs. 2 and 3 over a wide range of frequencies. We note the very close agreement for the nondegenerate eigenvalues, asso-

[7] Montgomery, Dicke, and Purcell, *op. cit.*, see pp. 427–428.

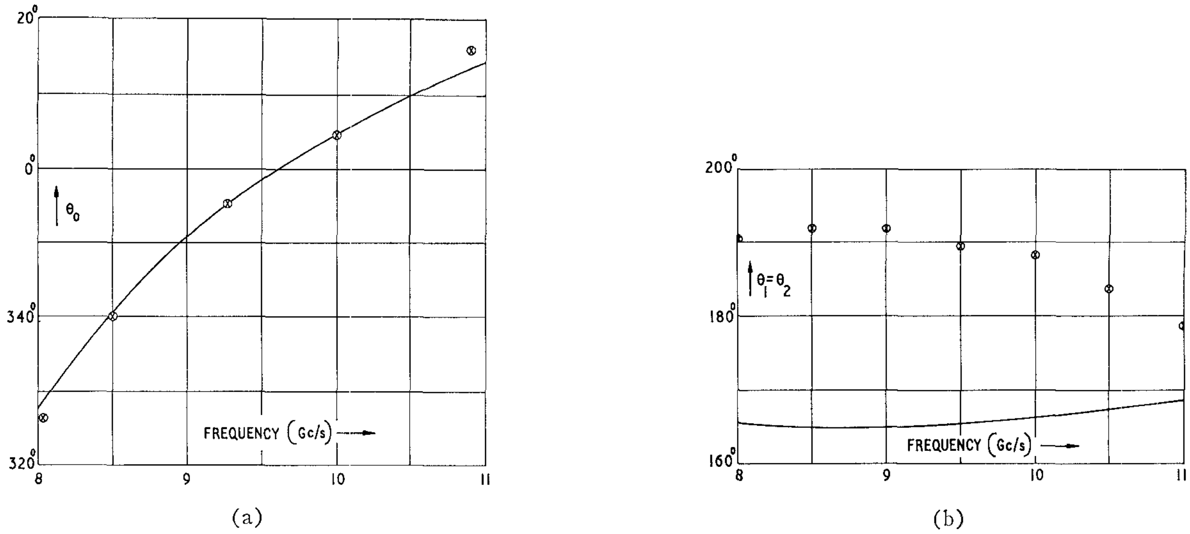

Fig. 2—Arguments of the scattering matrix eigenvalues for the empty 3-port junction. The frequencies given are for waveguide of internal broad dimension 0.9 in.

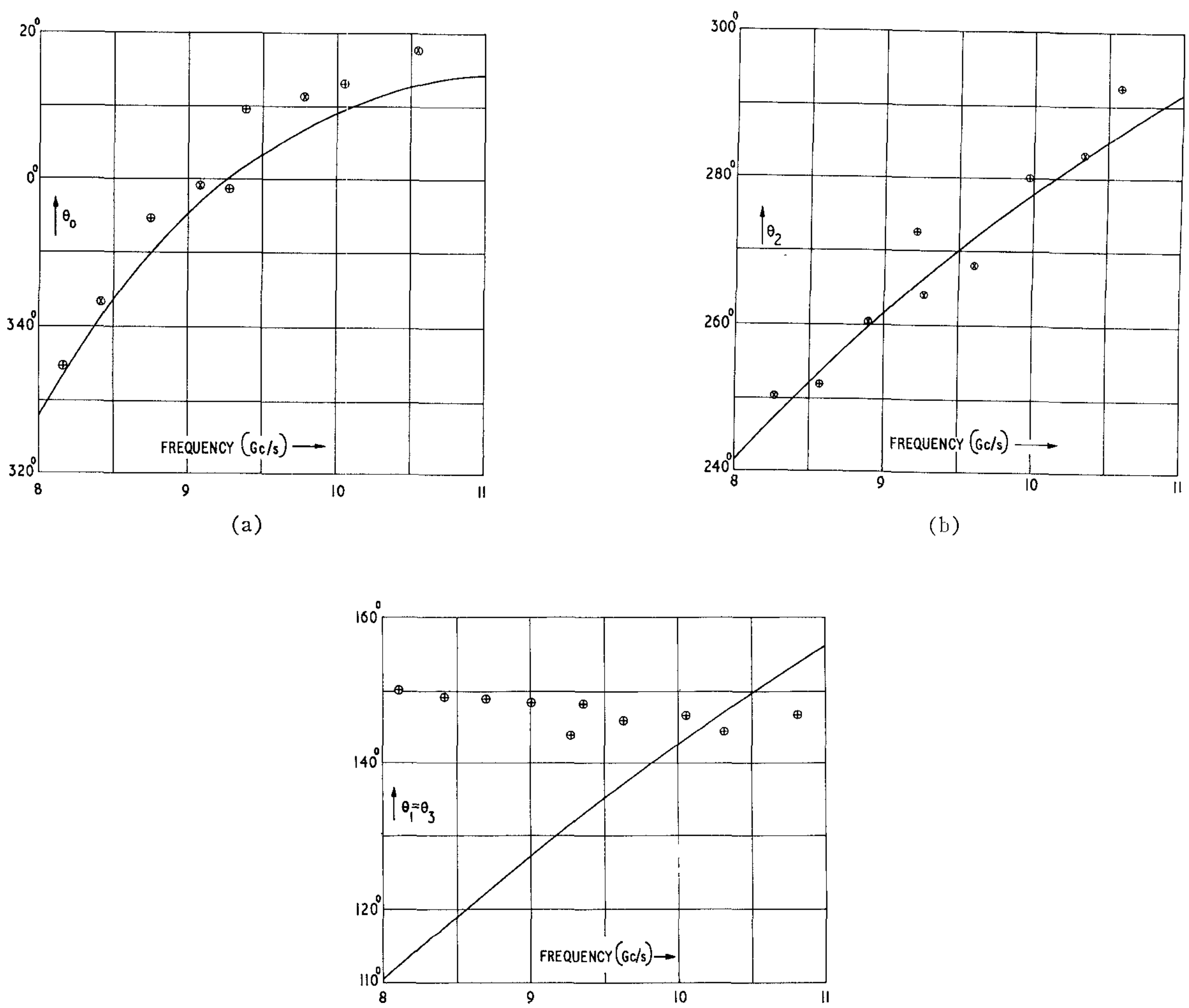

Fig. 3—Arguments of the scattering matrix eigenvalues for the empty 4-port junction. The frequencies given are for waveguide of internal broad dimension 0.9 in.

ciated with θ_0 (and with θ_2 for the 4-port junction). The cases of degenerate eigenvalues ($\theta_1=\theta_2$ and $\theta_1=\theta_3$) are, however, quite different. More will be said of this in Section VI, but it should be pointed out that even the worst disagreement between theory and experiment over the measured frequency range gives a useful result for the junction parameters.

Note that throughout this analysis the terminal planes have been at an integral number of half-wavelengths from the junction center, *i.e.*, are effectively planes through the junction center. Although mathematically convenient, this is not a physically realistic set of reference planes, and so Figs. 2 and 3 do not give eigenvalue arguments with the necessary monotonic decreasing dependence on frequency. Moving the planes into the waveguide proper in fact corrects this situation.

2) 4-Port Junction with Central Conducting Post:

The analysis can be applied to a junction with centrol conducting post, where in place of (14) we have:

$$\frac{C_n}{B_n} = \frac{-J_n(\gamma_0 R)}{Y_n(\gamma_0 R)}\,. \tag{38}$$

The following results in Table I have been obtained for a post diameter of 2/9 the rectangular guide width and at the frequency for which $\lambda_g=\lambda_c$.

TABLE I
4-Port Junction with Central Conducting Post

	θ_0	$\theta_1=\theta_3$	θ_2
Theory	96.12°	153.30°	266.88°
Experiment	97.5°	170.2°	265.6°
Difference	−1.4°	−17.9°	+1.3°

Again we note the very good agreement for the nondegenerate eigenvalues, but less accurate results for the degenerate case.

3) 2-Port Junction (viz. Straight Waveguide) with Thin Central Ferrite Post:

The analysis of Epstein and Berk,[8] although limited to a thin ferrite post, does give a rigorous result for the first order perturbation of the scattering matrix (or its eigenvalues) due to the ferrite in the waveguide. Their results in terms of the perturbed eigenvalues are

$$\lambda_0 = 1 - 2i(\gamma_0 R)^2\left[\frac{\epsilon}{\epsilon_0} - 1\right] \tag{39}$$

$$\lambda_1 = -1 - 2i(\gamma_0 R)^2\left[\frac{\mu_0^2 - \mu^2 + \kappa^2}{(\mu_0+\mu)^2 - \kappa^2}\right]. \tag{40}$$

[8] P. S. Epstein and A. D. Berk, "Ferrite post in a rectangular waveguide," *J. Appl. Phys.*, vol. 27, pp. 1328–1335; November, 1956.

The results of the analysis of this paper are

$$\lambda_0 = 1 - 1.978i(\gamma_0 R)^2\left[\frac{\epsilon}{\epsilon_0} - 1\right] \tag{41}$$

$$\lambda_1 = -1 - 1.760i(\gamma_0 R)^2\left[\frac{\mu_0^2 - \mu^2 + \kappa^2}{(\mu_0+\mu)^2 - \kappa^2}\right]. \tag{42}$$

The perturbation terms differ by 1.1 per cent and 12 per cent, respectively. The expression in the square brackets of (42) appears as the arithmetic mean of the two terms

$$\left[\frac{\mu_0 - (\mu \pm \kappa)}{\mu_0 + (\mu \pm \kappa)}\right],$$

this being the procedure explained in Section III for any junction with an even number of ports.

V. Application of the Analysis to Circulator Design

An approximate solution has been derived for the scattering matrix explicitly in terms of the geometry and electromagnetic properties of the junction. As the equations do not lend themselves to inversion, a particular microwave performance can only be arrived at by calculating the scattering matrix for some suitable set of values of the junction parameters. This procedure has been applied to the theoretical design of 3-port and 4-port circulators, employing a high-speed computer. In each case the scattering matrix has been calculated for ferrite post diameters from 0 to $3\lambda_0/2\pi$, with relative ferrite permeability tensor components μ/μ_0 from 0.5 to 1.0 and κ/μ_0 from 0 to 0.6. This range was taken to include typical tensor component values for ferrite well below resonant field. Calculations and experiments are for the frequency at which the guide and cutoff wavelengths are equal. All experiments are at 9273 Mc with waveguide of broad internal dimension 0.9 in.

A. The 3-Port Circulator

For the 3-port junction, perfect circulation is predicted over a small range of ferrite post radius, and the relation between μ, κ and ferrite radius for such circulation is given in Fig. 4. Given the practical dependence of μ on κ for varying applied magnetic field, Fig. 4 can be used to choose a suitable ferrite and post diameter. If we superimpose on the figure a curve of practical κ against μ for some possible ferrite, any intersection with the theoretical curve will give the appropriate μ and κ to be used, the figure also giving the ferrite post diameter. Applying this procedure at 9273 Mc two of the available ferrites were found suitable—Ferroxcube D5 with diameter 0.314 in and Ferroxcube 5D3 with diameter 0.323 in. The data on these ferrites are, however, subject to experimental errors of ±20 per

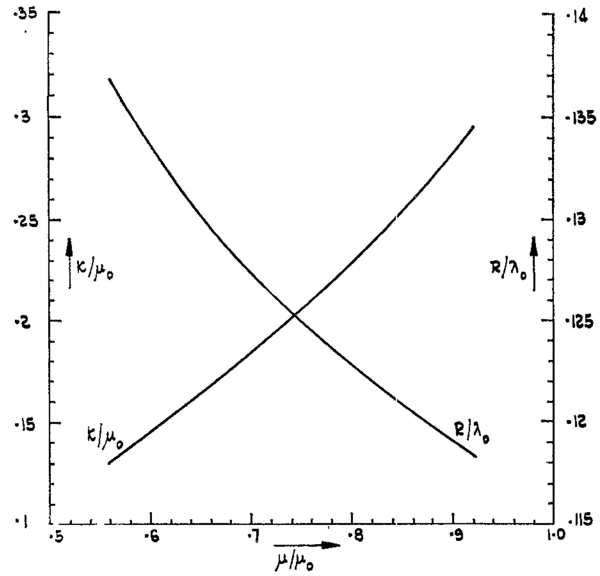

Fig. 4—Theoretical design data for the 3-port Y circulator.

cent and ± 10 per cent in μ and κ respectively, in addition to any variations between the different ferrite batches. Because the experimental data were based on thin ferrite disks, the required magnetic field could not be accurately predicted and the field had therefore to be adjusted for maximum isolation in all cases.

The practical junction with Ferroxcube 5D3 was found to give no conclusive results. For all magnetic fields giving any reasonable circulation the insertion loss was greater than 10 db, and of the incident power less than 20 per cent emerged from the junction. Whatever the loss mechanism in the ferrite, the analysis could not be expected to apply to such a lossy junction.

The junction with Ferroxcube D5 gave more satisfactory results. Although at the predicted diameter of 0.314 in the insertion loss was 8.2 db, the isolation was 10.8 db and the VSWR was 11, a small reduction of diameter, to 0.3085 in., gave an insertion loss of 0.8 db, an isolation of 11.7 db and a VSWR of 1.7. The practical dependence of circulator performance on post diameter is shown in Fig. 5.

B. The 4-Port Circulator

In the 3-port junction, where two conditions have to be satisfied, we find a continuous (but narrow) range of μ, κ, R values consistent with circulation. For the 4-port junction, none of the μ, κ, R values computed gives rise to a circulator, and so a convenient fourth variable must be introduced. In place of the central post of homogeneous ferrite we consider a post in sandwich form, consisting of many thin ferrite disks interspaced by thin conducting disks. It is assumed that the ferrite disks are so thin as to support no propagating modes with z dependence. The fields within the ferrite will be given by (4)–(7) and outside the post by (8)–(11). We ignore the fringing fields and match at $r=R$ the

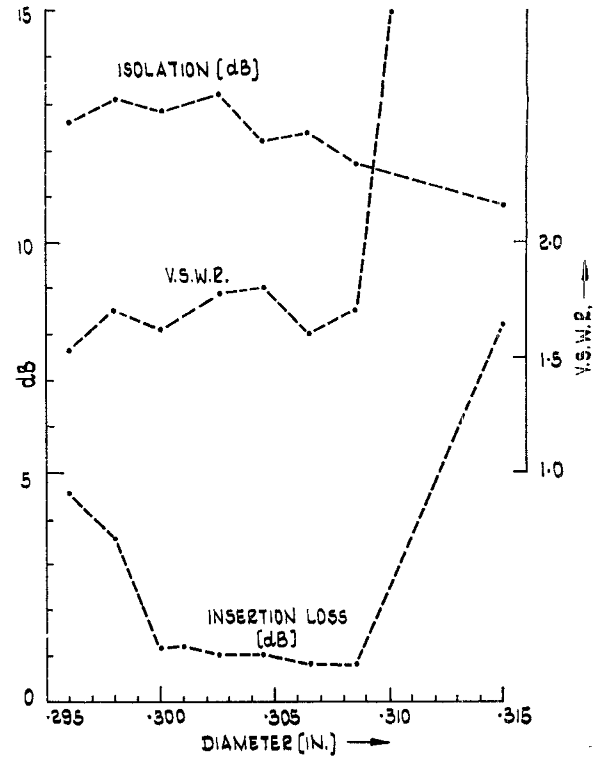

Fig. 5—Experimental performance of a Y circulator with Ferroxcube D5 at 9273 Mc, with a predicted optimum diameter of 0.314 in.

values of E_z and H_ϕ averaged in the z direction. Eq. (13) remains unchanged, but (12) is modified to

$$\eta A_n J_n(\gamma R) = B_n J_n(\gamma_0 R) + C_n Y_n(\gamma_0 R) \qquad (43)$$

where

$$\eta = \frac{\text{total ferrite thickness}}{\text{total ferrite and conductor thickness}}.$$

Eq. (14) now becomes

$$\frac{C_n}{B_n} = -\frac{J_n(\gamma_0 R)}{Y_n(\gamma_0 R)} \cdot \frac{\left\{\left[\frac{J_n'(R)}{\gamma R J_n(\gamma R)} + \frac{\kappa n}{\mu(\gamma R)^2}\right]\frac{\epsilon}{\epsilon_0} - \frac{\eta J_n'(\gamma_0 R)}{\gamma_0 R J_n(\gamma_0 R)}\right\}}{\left\{\left[\frac{J_n'(\gamma R)}{\gamma R J_n(\gamma R)} + \frac{\kappa n}{\mu(\gamma R)^2}\right]\frac{\epsilon}{\epsilon_0} - \frac{\eta Y_n'(\gamma_0 R)}{\gamma_0 R Y_n(\gamma_0 R)}\right\}}. \qquad (44)$$

The analysis is therefore extended to the case of the central post with interspaced ferrite/conducting disks by using (44) in place of (14) for insertion in (30).

This procedure has been applied to the 4-port junction in which η takes values 0.75, 0.5 and 0.25. Whilst no perfect circulator is predicted, a number of "near-circulators" are predicted with μ's and κ's corresponding to the approximate practical values of available ferrites. Four junctions have been made to these designs and their measured performances are given in Table II. The measured and predicted figures are shown for comparison, although the most important point is that these practical figures have been obtained from purely theoretical designs, with the theoretical figures indicating the ultimate that could be expected.

TABLE II

		Experiment	Theory
Ferroxcube 5B1: Diameter 0.263 in $\eta=0.25$ in	V.S.W.R.	1.75	1.31
	Isolation	20.5 db	18.9 db
	Cross-coupling	11.0 db	18.9 db
	Insertion-loss	1.1 db	0.25 db
Diameter 0.283 in $\eta=0.25$	V.S.W.R.	2.26	1.46
	Isolation	24.9 db	19.8 db
	Cross-coupling	16.1 db	15.4 db
	Insertion-loss	1.9 db	0.4 db
Ferroxcube D5: Diameter 0.303 in $\eta=0.25$	V.S.W.R.	1.97	1.61
	Isolation	30.6 db	20.2 db
	Cross-coupling	14.1 db	14.0 db
	Insertion-loss	1.4 db	0.5 db
Diameter 0.323 in $\eta=0.5$	V.S.W.R.	2.0	1.58
	Isolation	14.4 db	13.0 db
	Cross-coupling	14.3 db	13.0 db
	Insertion-loss	1.8 db	0.7 db

VI. Discussion on the Accuracy of the Approximate Analysis

As mentioned in Section IV, the most precise testing of the theory has been with experiment for reciprocal junctions and with existing theory for the thin ferrite post in waveguide. Less precise, but perhaps of more practical importance, are the measurements on circulators predicted theoretically.

Agreement between the theory and experiment of the reciprocal junctions is very good for θ_0 of the 3-port and θ_0 and θ_2 of the 4-port, but is by no means as good for the other eigenvalues. The distinct difference is presumably because of the two-fold degeneracy of θ_1 with θ_2 or θ_3. An alternative distinction is that in one case the eigenvalues have associated eigenvectors with real elements whereas the other eigenvectors have complex elements. For instance, eigenvectors (1, 1, 1, 1), (1, −1, 1, −1), (1, i, −1, −i) and (1, −i, −1, i) have been used in the analysis of the 4-port. The degenerate eigenvalues with arguments $\theta_1=\theta_3$ can, however, have (1, 0, −1, 0) and (0, 1, 0, −1) as their associated eigenvectors. Repeating the field analysis of Section III for these different eigenvectors gives exactly the same result as before. It therefore appears that the difference in accuracy between the various eigenvalues is due primarily to the degeneracy, the result being typical of any approximation to a degenerate system in mathematical physics. If this is so, we can expect the approximate analysis to be fairly accurate (to within say 5° of eigenvalue argument) for nonreciprocal junctions. The evidence of Section V (in particular that of Table II) tends to support this expectation.

VII. Conclusions

The analysis given can be applied to the m-port waveguide junction when empty, or with a central post of ferrite, dielectric or conducting material. Comparison of theory with experiment for reciprocal 3- and 4-port junctions gives close agreement except for the inherently degenerate eigenvalues of the scattering matrix. It is believed that the analysis will be accurate for all eigenvalues when the junction is significantly nonreciprocal, and this belief is supported by the fair success in the theoretical design of 3- and 4-port circulators.

It should be emphasized that only the difficulties of computing limit the accuracy of the analysis or any extension of it to other configurations. The accuracy of the analysis can always be improved by taking successive approximations to the infinite system of (26).

VIII. Appendix

The factors D_n^m, E_n^m, F_n^m, G_n^m defined by (31) to (34) are shown in Table III for application to 2-, 3- and 4-port junctions when the (rectangular) guide and cutoff wavelengths are equal.

The author has copies available of the computed D, E, F and G (and of θ for the empty junction) for 3- and 4-port junctions over the range of frequencies 8–11 Gc/s for 0.9-in waveguide.

TABLE III

m	n	D_n^m	E_n^m	F_n^m	G_n^m
2	0	−.3574802	+.1482101	0	+.4501582
2	1	0	+.3183099	+.2841222	+.0609223
3	0	−.3106360	+.0522288	−.0131288	+.2319510
3	1	−.0266972	+.2698898	+.2060289	+.0459024
4	0	−.2144655	−.0394135	0	+.1591549
4	1	−.0684786	+.1864479	+.1516500	+.0278695
4	2	+.0905958	+.1142328	+.0968433	−.1045223

IX. Acknowledgment

The author wishes to thank Drs. Ir. A. J. W. Duijvestijn and Ir. W. Fontein of the Philips Computing Centre, Eindhoven, The Netherlands, for much of the programming and computing concerned with this analysis. Acknowledgment is also made to the Director of Mullard Research Laboratories for permission to publish the paper.